Processing and Application of Ceramics 4 [3] (2010) 147–156

Nanoferroelectric perovskite oxides with unusual morphology produced by different synthesis procedures

Alessio Bassano[1], Vishwanath Kalayani[1,2], Lavinia P. Curecheriu[3], Maria T. Buscaglia[1], Vincenzo Buscaglia[1], Liliana Mitoseriu[3], Paolo Nanni[1,2,*]

[1]*Institute for Energetics and Interphases, National Research Council, Via De Marini 6, I-16149 Genoa, Italy*
[2]*Department of Chemical & Process Engineering, University of Genoa, P.le Kennedy, I-16129 Genoa, Italy*
[3]*Department of Physics, "Al.I. Cuza" University, Blvd. Carol I, Ro 700506 Iasi, Romania*

Received 4 February 2010; received in revised form 18 May 2010; accepted 21 July 2010

Abstract

We report in the present paper some original results of a joint research performed in the framework of the COST Action 539 ELENA. In search of higher miniaturisation of electroceramic devices a new outlook seems to arise from ceramics with unusual morphology that might present a new kind of circular or toroidal ferroelectric ordering of dipoles. Completely new perspectives in data storage can be expected if a close control of size confinement and dimensionality as well as of the chemical composition and the phase purity is reached. We succeeded in the fabrication of $BaTiO_3$ hollow nanoparticles and nanowires, and $Bi_4Ti_3O_{12}$ platelets. The use of soft chemistry and solid state methods allowed to produce coreshell powders and ferroelectric-ferromagnetic composites with completely new functional properties.

Keywords: *ferroelectric, core-shell, nanoparticles, nanowires*

I. Introduction

Ferroelectric perovskites-like oxides exhibit a wide field of applications as electroceramics due to their versatility that makes them employed as MLCCs (Multy-Layer Ceramic Capacitors), NFERAMs (non-volatile ferroelectric random access memories), PTCR (positive temperature coefficient of resistance) thermistors, piezoelectric transducers and actuators, pyroelectric sensors and electro-optic devices [1–3]. Some of them also find tunable microwave application due to their high dielectric constant (ε_r), strong dependence of ε_r on the applied field, and low losses [4].

In the last few years, an increasing attention was focused on the synthesis of ferroelectric precursors with unusual micro/nanoscale morphology such as spheres, cubes, disks, rods, rings, ribbons, tubes, and hollow particles as well as regular arrays of these structural units [2,5–7]. The reason of this interest is related to the possibility of reaching a deeper understanding of ferroelectric and switching properties in 1D, 2D and 3D small structures which in turn should allow a significant improvement in the fabrication of next generation of fully three-dimensional NFERAMs structures at high bit density [2]. Moreover, some fundamental aspects not completely elucidated, such as the mechanism of formation and arrangement of domains in ferroelectric nanostructures, might be clarified. A further explanation for such an interest is subsequent to the work of Naumov, Bellaiche and Fu [8] that performed detailed *ab initio* calculations of $Pb(Zr,Ti)O_3$ solid solutions from which a new kind of ferroelectric order in 1D or 2D systems was envisaged, i.e. circular or toroidal ordering of dipoles, that could open completely new perspectives in data storage [9,10].

Up to now advances in application of these nanomaterials moved forward rather slowly as a consequence of the difficulty in finding reliable techniques of fabrication with a close control of size confinement and dimensionality as well as of the chemical composition and the phase purity. In fact while the formation of nanostructures via template is fairly simple, the synthesis by chemical or solution methods are rather complex and literature data are not so abundant

* Corresponding author: tel: +39 010 6475 701
fax: +39 010 6475 700, e-mail: *p.nanni@ge.ieni.cnr.it*

(e.g. hydrothermal or solvothermal processing [11–14]). Relatively few papers have also been published on $BaTiO_3$, in spite its possible industrial interest [15–21]. Recently some works based on the possibility to use Kirkendall effect and diffusion processes in order to produce nanotubes and hollow nanoparticles were published [22–25].

In the present paper we report some original results obtained in the framework of the COST Action 539 ELENA. We succeeded in preparing $BaTiO_3$ as hollow nanoparticles and nanowires, and $Bi_4Ti_3O_{12}$ platelets. An extension of pure compounds preparation is the synthesis of core-shell powders by combining soft chemistry and solid state methods: various perovskites were prepared with possible applications when sintered to give local graded composition.

II. Experimental

2.1 Synthesis of $BaTiO_3$ core-shell particles

$BaTiO_3$ coated with $SrTiO_3$

Solid $SrCl_2 \cdot 6H_2O$ was added to a $TiOCl_2$ mother solution in the amount required to get Sr/Ti molar ratio 1.04. The quantity to be used being determined by the amount of ST needed to coat the BT cores [26]. The process was carried out in a closed PTFE vessel in order to avoid CO_2 adsorption from air with the consequent formation of carbonates. BT core particles were dispersed to form a thick slurry in a NaOH aqueous solution that maintains $[OH^-] \approx 1.0$ mol/L after quantitative precipitation of ST. The chloride solution was quickly added to the slurry under vigorous stirring. As the reaction is rather exothermic, the temperature raised up to ≈80°C. The slurry was eventually kept for 4 h at 90°C while stirring in a thermostatic bath.

$BaTiO_3$ coated with Y_2O_3

The synthesis procedure is similar to the one described by Kawahashi and Matijevic [27] for the coating of polystyrene submicron spheres with yttrium basic carbonate. In a typical synthesis, BT powder was suspended in deionised water inside a polypropylene bottle while stirring. $Y(NO_3)_3 \cdot 6H_2O$ and urea were added in a weight ratio ≈ 1 : 8. The $[Y^{3+}]/[BaTiO_3]$ molar ratio was 0.2. The suspension was heated up to 95°C at 1 °C/min in a thermostatic bath and kept at the final temperature for 3 h under stirring [28].

(Ni,Zn)Fe_2O_4 coated with $BaTiO_3$

Composite particles, consisting of a $Ni_{0.5}Zn_{0.5}Fe_2O_4$ core (produced by EPCOS) and $BaTiO_3$ shell were obtained. Firstly, a uniform layer of amorphous titania has been formed on the surface of fine ferrite particles suspended in a peroxotitanium (IV) solution by a precipitation process. A suspension of nanocrystalline $BaCO_3$ prepared in water was slowly added to the suspension containing the (Ni,Zn)Fe_2O_4@TiO_2 particles. The formation of the $BaTiO_3$ single phase shell from the TiO_2@$BaCO_3$ occurs by a single step reaction at 800°C for 1 hour. As result, composite fine powders of (Ni,Zn)Fe_2O_4 @$BaTiO_3$ with narrow size distribution, and without agglomerates were obtained. The mixture was then milled, isostatically pressed and sintered at 1050–1150°C for 1 hour to result in di-phase magnetoelectric ceramic composites.

2.2 Synthesis of $BaTiO_3$ hollow particles

Core-shell particles consisting of $BaCO_3$ core and TiO_2 shell, were obtained by suspending a $BaCO_3$ powder (Solvay Bario e Derivati, specific surface area 3.3 m^2/g) in an aqueous solution of peroxytitanium (IV) [29]. The $BaCO_3$ powder comprises elongated crystals (0.2–1.5 μm with 0.2–0.6 μm diameter). Formation of the coating was obtained by slowly heating the suspension up to 95°C, keeping at constant temperature for 5 h. The Ba/Ti molar ratio in the suspension was 1.0. The as-prepared coated powders were fired in air at 700°C with a heating rate of 5 °C/min an isothermal treated for 24 h.

2.3 Synthesis of $BaTiO_3$ nanowires

Fabrication of the $BaTiO_3$ NWs was carried using a three step procedure [30]: i) synthesis of layered titania nanowires; ii) coating of the titania NWs with nanocrystalline $BaCO_3$; iii) solid state reaction at 700°C.

i) *Synthesis of layered titania nanowires.* In a typical synthesis, ultrafine TiO_2 powder (VP TiO_2 P 90, Degussa) was dispersed in 10M NaOH solution while vigorous stirring. The resulting suspension was transferred in a stainless steel PTFElined autoclave heated at 250°C for 5 h. The resulting precipitate, consisting of $Na_2Ti_4O_9$ NWs, was collected, washed several times alternatively with distilled water and a 1M HNO_3 solution, and finally aged overnight at pH 1 under stirring. This treatment determined the transformation of sodium titanate into layered hydrous titania nanowires (TNWs) by ion exchange that preserved the morphology of the starting NWs. The precipitate was then washed with a 0.1M HNO_3 solution by centrifugation and re-dispersed again in the HNO_3 solution using a ultrasonication horn. The resulting stable suspension was eventually freeze-dried resulting in a white and fluffy powder.

ii) *Coating of titania nanowires with $BaCO_3$.* Very fine $BaCO_3$ powder (Solvay Bario e Derivati) was dispersed in a dilute NH_4OH solution at pH 8 by prolonged ultrasonication. A suspension of TNWs precursor was also prepared following the same procedure and heated at 90°C. The $BaCO_3$ suspension was then slowly added to the TiO_2 suspension while stirring. After complete addition, the suspension was kept at 90°C for 30 min resulting in a shell deposition of $BaCO_3$ onto TiO_2.

iii) *Solid-state reaction*. The TiO_2-$BaCO_3$ core-shell powder was finally put in a platinum crucible and calcined in air (6h; 700°C).

2.4 Synthesis of $Bi_4Ti_3O_{12}$ nanoplates and nanowires

$Bi_4Ti_3O_{12}$ nanoplates were synthesized by hydrothermal method using Bi_2O_3 and titanium *tert*-butoxide [TTB, $Ti(OC_4H_9)_4$] as starting materials, NaOH served as a mineraliser and polyethylene glycol (PEG) as additive. The typical procedure started with the preparation of a homogenous slurry (A) by adding Bi_2O_3 in ethanol under stirring for 20 min. A second solution (B) was formed by dissolving $Ti(OC_4H_9)_4$ in ethanol, again stirring for several minutes. Afterwards, the B solution was slowly dropped into the A solution at constant rate, stirring for 30 min. In the following step, a NaOH solution together with a PEG solution was dropped into the A-B mixture under vigorous stirred. Finally, the mixture was poured into a Teflon vessel and diluted with distilled water. The vessel was then placed into a stainless steel tank to perform the hydrothermal treatment at 200°C for different reaction times.

2.5 Characterisation

After the synthesis, the final products were opportunely treated to undergo a standard characterisation. Thus, they were observed by scanning electron microscopy (SEM) whereas the phase composition was determined by conventional X-ray diffraction (XRD). The density, ρ, was measured by helium picnometry and the specific surface area (S_{BET}) was determined by nitrogen physisorption (BET) from which the equivalent BET diameter was calculated (d_{BET}). Phase purity was investigated by XRD and the crystallite size (d_{XRD}) was estimated from the broadening of the XRD peaks by means

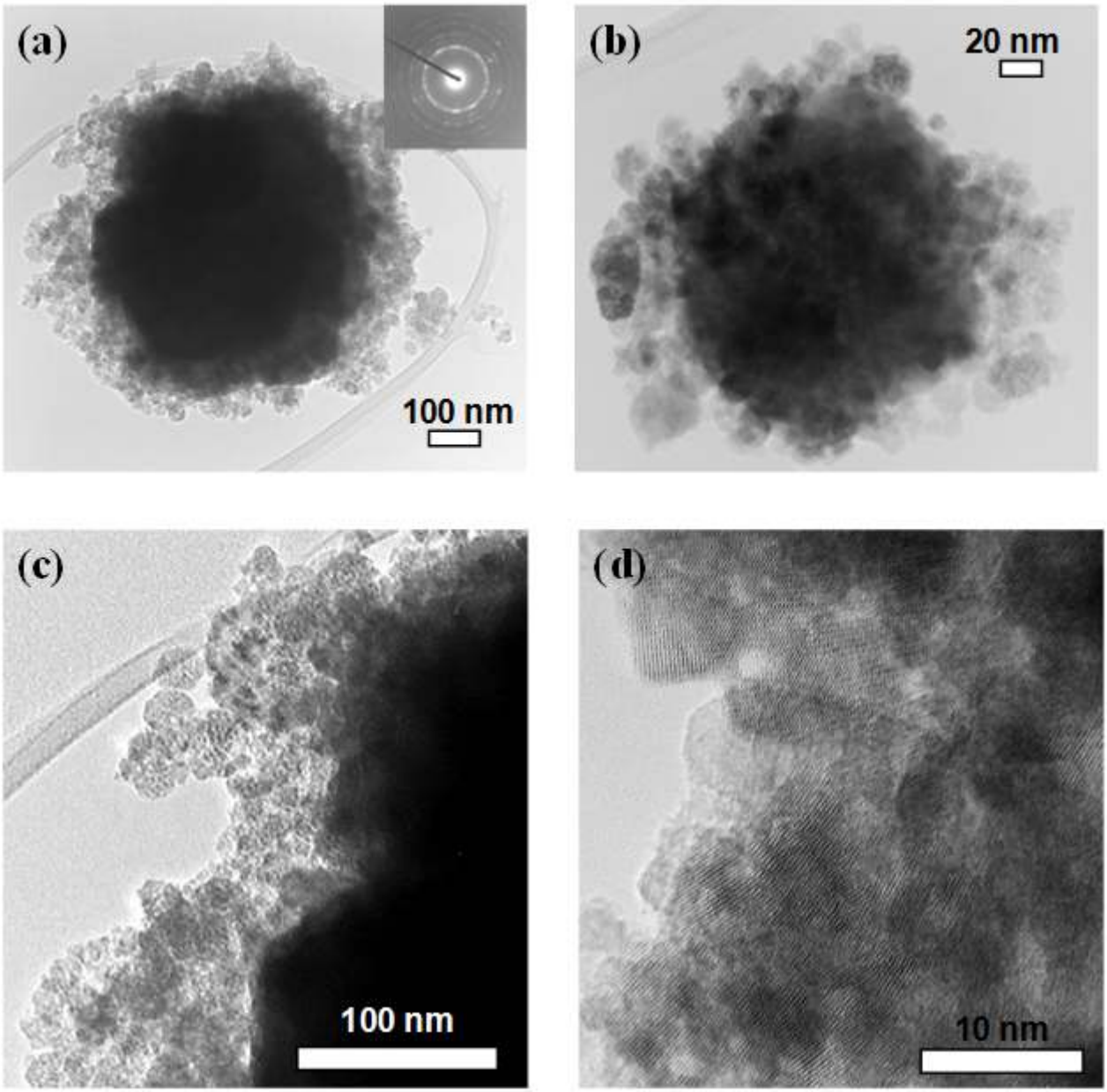

Figure 1. $BaTiO_3$ particles coated with $SrTiO_3$. (a) TEM image of a typical core-shell particle with diameter of $BaTiO_3$ core of 500 nm. (b) TEM image of a typical core-shell particle with diameter of $BaTiO_3$ core of 200 nm. (c,d) High-resolution TEM images of $SrTiO_3$ nanocrystals of the shell. The ED pattern shown in the inset of part (a) shows that the orientation of the $SrTiO_3$ nanocrystals is almost random.

of the Scherrer equation, after instrumental correction with a Si standard, assuming negligible microstrain broadening. The internal structure of the particles and the coatings were studied by high-resolution transmission electron microscopy (HRTEM) and by electron diffraction (ED).

III. Results and discussion

$BaTiO_3$-core $SrTiO_3$-shell

To show the versatility of the coating method, BT cores of different size (≈200 and ≈500 nm) were used to prepare core-shell particles [26] with nominal compositions $Ba_{0.64}Sr_{0.36}TiO_3$ (BT core 500 nm) and $Ba_{0.44}Sr_{0.56}TiO_3$ (BT core 200 nm). Direct evidence of the growth of a ST shell onto BT core is provided by TEM images (Fig. 1a,b) that show a granular coating made up of ≈10 nm faceted ST nanocrystals (Fig. 1c,d). Observations at high resolution and ED show that most of the ST nanocrystals in the coating layer are randomly oriented. Further evidence of the presence of coating was given by energy-dispersive X-ray analysis which revealed the presence of Sr at the surface of the particles. XRD patterns of the as-prepared core-shell particles show that the spectra of the coated powders exact-

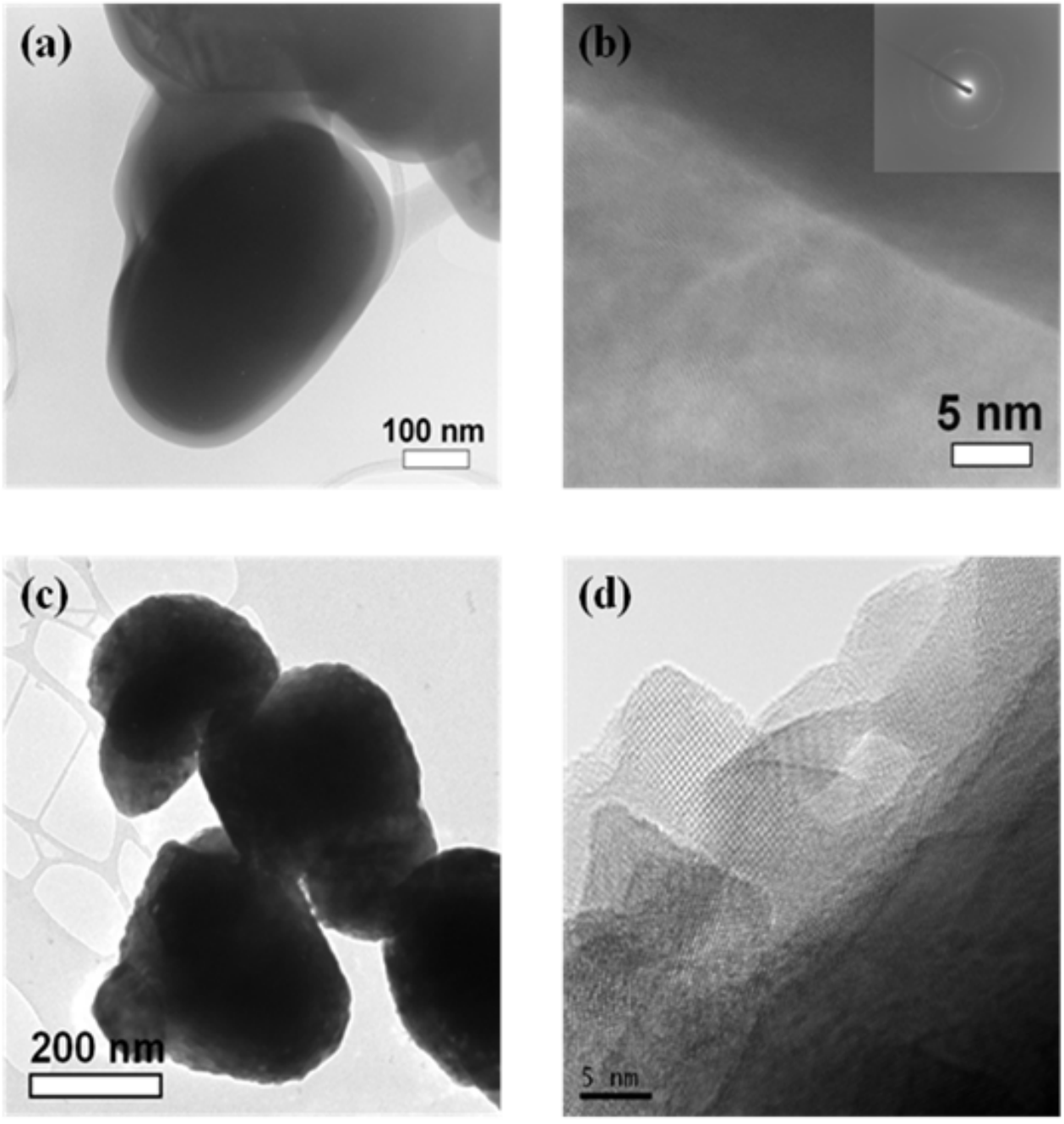

Figure 2. $BaTiO_3$ particles coated with yttrium basic carbonate. (a,b) As-coated particles. Part a: low-resolution TEM image. Part b: high-resolution TEM image of the shell region. The inset shows the ED pattern of the shell. (c,d) High-resolution TEM images of the shell region of particles calcined at 700°C.

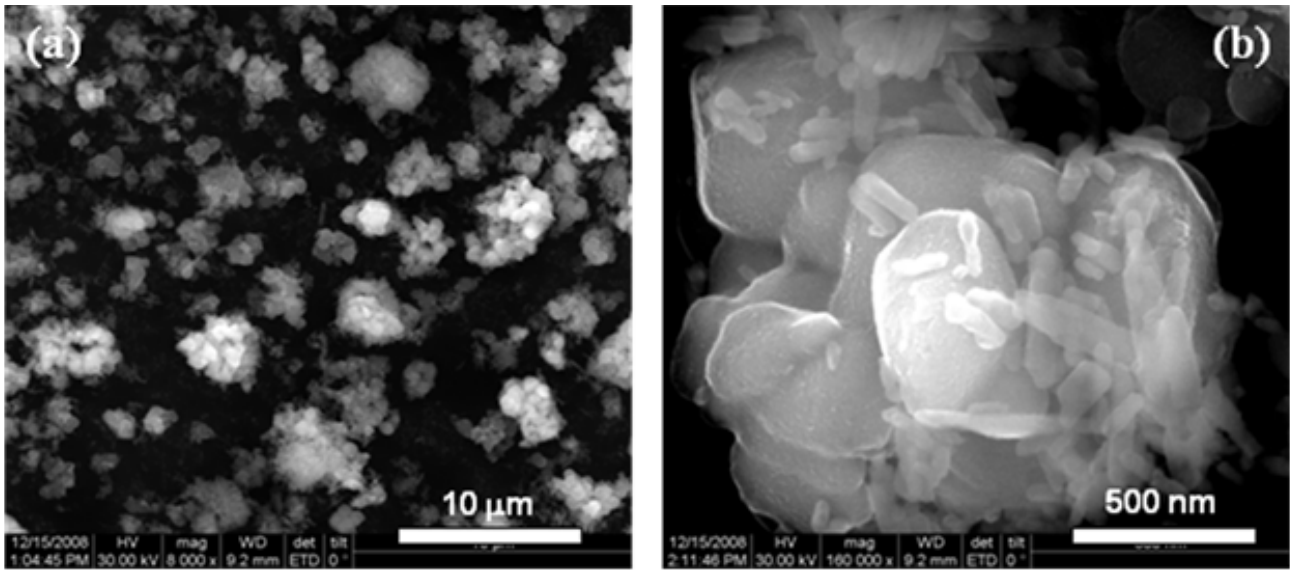

Figure 3. SEM-FEG images of the $NiZnFe_2O_4$-$BaTiO_3$ composite powders with core-shell structure obtained after calcinations at 800°C for 1 hour: (a) general view; (b) higher magnification view. Beside the formation of nanocrystalline shell onto the $(Ni,Zn)Fe_2O_4$ core, $BaTiO_3$ is formed also as 1D-structures.

ly correspond to the superposition of the patterns of the parent perovskites, free of any other phase [31].

$BaTiO_3$-core Y_2O_3-shell

TEM observations (Fig. 2a) shown the formation of a homogeneous and smooth coating ≈20 nm thick [28]. The shell was made up of an Y compound, as revealed by EDS analysis. However, only pure BT reflections were observed in the XRD pattern of the as-coated powder, indicating that the shell was mainly amorphous or poorly crystalline. In fact, according to HRTEM (Fig. 2b), the shell region was composed of small nanocrystals (≈5 nm) dispersed into an amorphous matrix. In order to determine the composition of the shell, the precipitation of the Y compound was performed in the same experimental conditions without BT particles giving rise to spherical particles with a uniform diameter of ≈300 nm. The XRD pattern displayed only three weak and very broad peaks indicating a predominantly amorphous phase that comprises very small crystallites (few nm in size). Thermogravimetric data demonstrated that the particles were composed of yttrium basic carbonate, $Y(OH)CO_3 \cdot H_2O$ (YBC), according to Matijevic findings [32] and therefore it can be assumed that the shell grew on BT cores correspond to the same compound. Calcination at 700°C for 2 h resulted in the decomposition of YBC toY_2O_3 with cubic bixbyte structure. Typical HRTEM images of the shell region after calcination (Fig. 2c,d) showed a continuous and relatively smooth coating of Y_2O_3 nanocrystals (5–15 nm).

$(Ni,Zn)Fe_2O_4$-core $BaTiO_3$-shell

The low magnification SEM-FEG image of the core-shell $(Ni,Zn)Fe_2O_4$@$BaTiO_3$ powder resulted after calcination at 800°C/1h shows the formation of non-uniform agglomerates of ~ 3–4 µm (Fig. 3a). The higher magni-

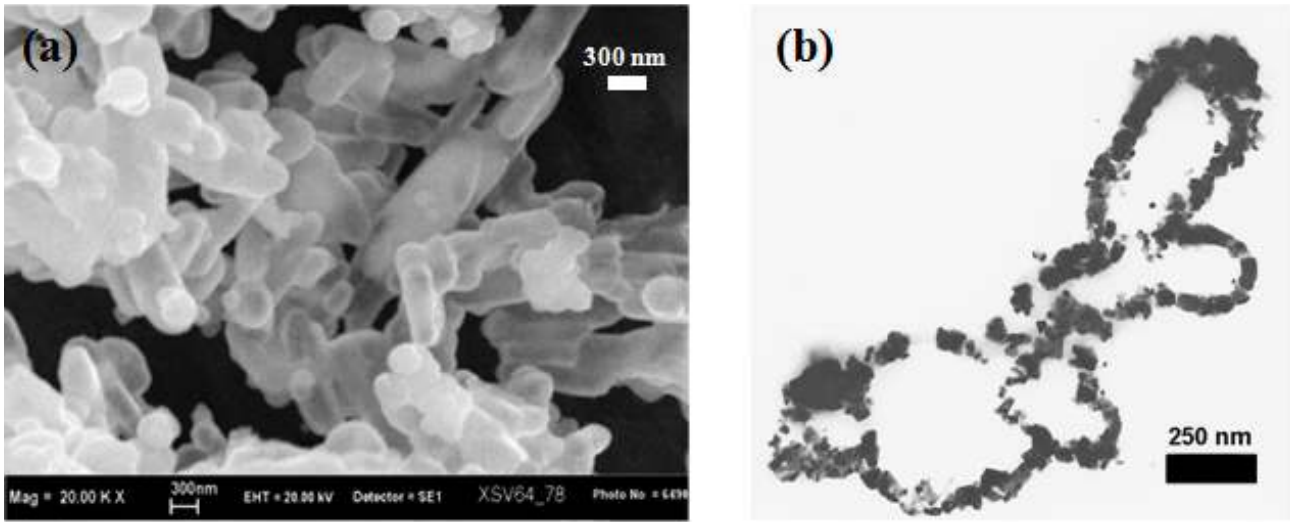

Figure 4. (a) SEM image of $BaTiO_3$ hollow particles obtained after 4 h calcination at 700°C and (b) TEM image of the cross-section of the same $BaTiO_3$ hollow particles

fication images (Fig. 3b) indicate that these aggregates consist of particles with two different morphologies, i.e. almost spherical interconnected ferrite particles with an average size of 600 nm covered by smaller, needle-like $BaTiO_3$ particles exhibiting an average length of 130 nm and an average diameter of 57 nm. These composite powders have been used to prepare di-phase ceramic composites with magnetoelectric properties, by choosing an appropriate sintering strategy.

$BaTiO_3$ hollow particles

The general morphology of the precursor $BaCO_3$, the $BaCO_3$-TiO_2 core shell powder and the final BT hollow particles obtained after calcination remained practically unchanged during the different fabrication steps [29]. The surfaces of the final particles were free of evident holes and cracks (Fig. 4a). Convincing proof of the formation of BT hollow particles obtained according our production method was provided by TEM investigations (Fig. 4b). The particles after dispersion in a matrix, were cut in slices and the cross-sections distinctly shown a rather uniform empty layer (average thickness ≈70 nm) corresponding to the initial shell, composed of equiaxed nanocrystals. The dimension of the hollow particles is comparable to the one of original $BaCO_3$. Because of the relatively high reaction temperature, the final hollow particles resulted aggregates. In a previous study [33], $BaCO_3$ nanocrystals (length 100–500 nm, diameter 30–50 nm) were used for the coating process. However, hollow particles could not be obtained, because spontaneous fragmentation and collapse of the thin shell rapidly occurred already at temperatures below 600°C, i.e. before the complete formation of $BaTiO_3$. In that case, calcination at 700°C resulted in a fine powder composed of solid nanoparticles (≈25–50 nm). When the radius of the cavity was increased to 300–400 nm, as in the present case, the hollow structure could be aged at 700°C for quite a long time without evident deterioration. Therefore, the selection of core crystals with a suitable size and of the reaction temperature is of crucial importance in the solid-state fabrication of hollow structures.

$BaTiO_3$ nanowires

The diffraction pattern of TNWs obtained by acidic washing is reported in Figure 5a and it is similar to the ones reported for $H_2Ti_3O_7$, $H_2Ti_2O_5{\cdot}H_2O$ and titanates with lepidocrocite structure [34]. The diffraction pattern of the nanowires calcined at 700°C (Fig. 5b) corresponds to anatase single phase. The strongest peak at about 12.6° 2θ in Fig. 5a should correspond to the distance (0.82 nm) between two adjacent layers of TiO_6 octahedra. The weight loss at 600°C of the freeze dried powder closely matches with that expected for the compound $H_2Ti_2O_5{\cdot}H_2O$.

The morphology of the TNWs is shown in Fig. 6a,b. The fiber-like crystals have a width of 30–250 nm and a length from a few microns to >10 μm. The cross-section is rectangular, with a thickness of the order of several tens of nanometres. The high-resolution image of Fig. 6b indicates the single crystal nature of the TNWs. The lattice fringes are parallel to the elongation direction of the crystals with a separation of about 0.7 nm. This separation corresponds to the interlayer distance observed by HRTEM in $H_2Ti_3O_7$ and $H_2Ti_2O_5{\cdot}H_2O$ nanotubes [34,35]. Representative SEM and TEM images of the $BaTiO_3$.

NWs are reported in Fig. 6c-f. The NWs have a width between 50 and 300 nm and a length of 2–30 μm. In the case of NWs with regular morphology, ED patterns taken at different distances along the same NW showed the same diffraction pattern with sharp diffraction spots as evident in the inset of Fig. 6d: this is a proof of the single crystals nature of these NWs.

The most frequently observed lattice fringes are oriented parallel to the major axis of the nanowires and show a separation of about 0.27 nm (Fig. 6e). This

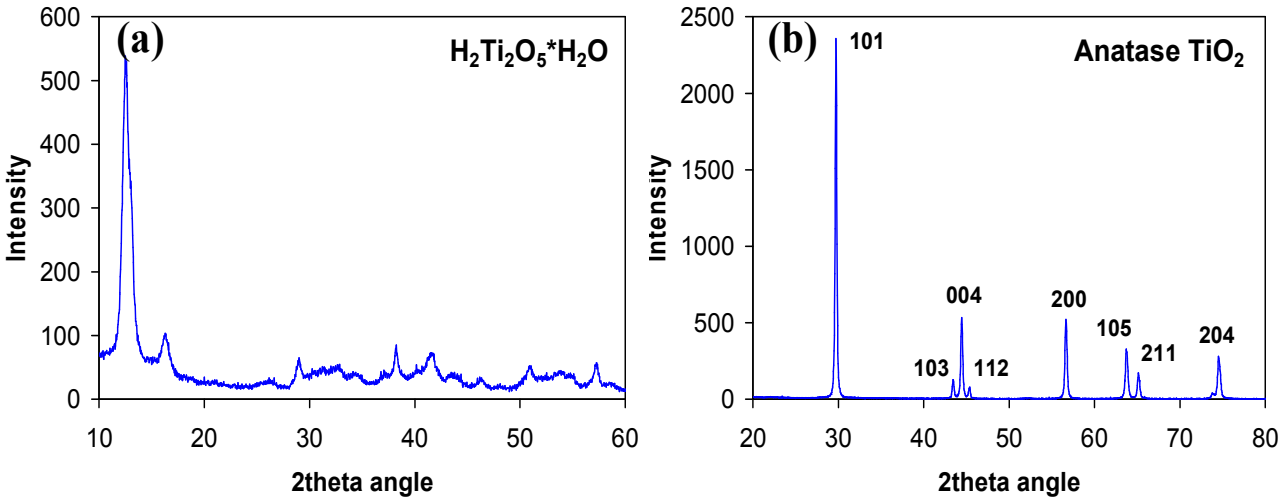

Figure 5. XRD patterns (Co Kα radiation) of (a) $H_2Ti_2O_5{\cdot}H_2O$ nanowires and (b) titania nanowires after calcination at 700°C

distance matches very well with the separation of the (110), (101) and (011) planes of $BaTiO_3$ (0.28 nm, ICDD PDF 5-0626). As a consequence, the elongation direction of the nanowires is perpendicular to one of the above directions.

NWs with less regular morphology are comprised two or more segments. Protuberances are often observed on the NW surface, as shown in Fig. 6d. EDS analysis indicated that the majority of the protuberances are composed of a barium compound, most likely $BaCO_3$. Dislocations, grain boundaries and internal pores (see Fig. 6f) were also detected inside the NWs.

$Bi_4Ti_3O_{12}$ nanoplates and nanowires

The morphology of the dried powder was characterised by SEM and the phase structure by XRD. The effects on the morphology of the reaction products were investigated as a function of some parameters like precursor's composition, reaction and aging time, temperature, PEG and base concentration. SEM images (Fig. 7a,b) shown that the condition for the nanowires forma-

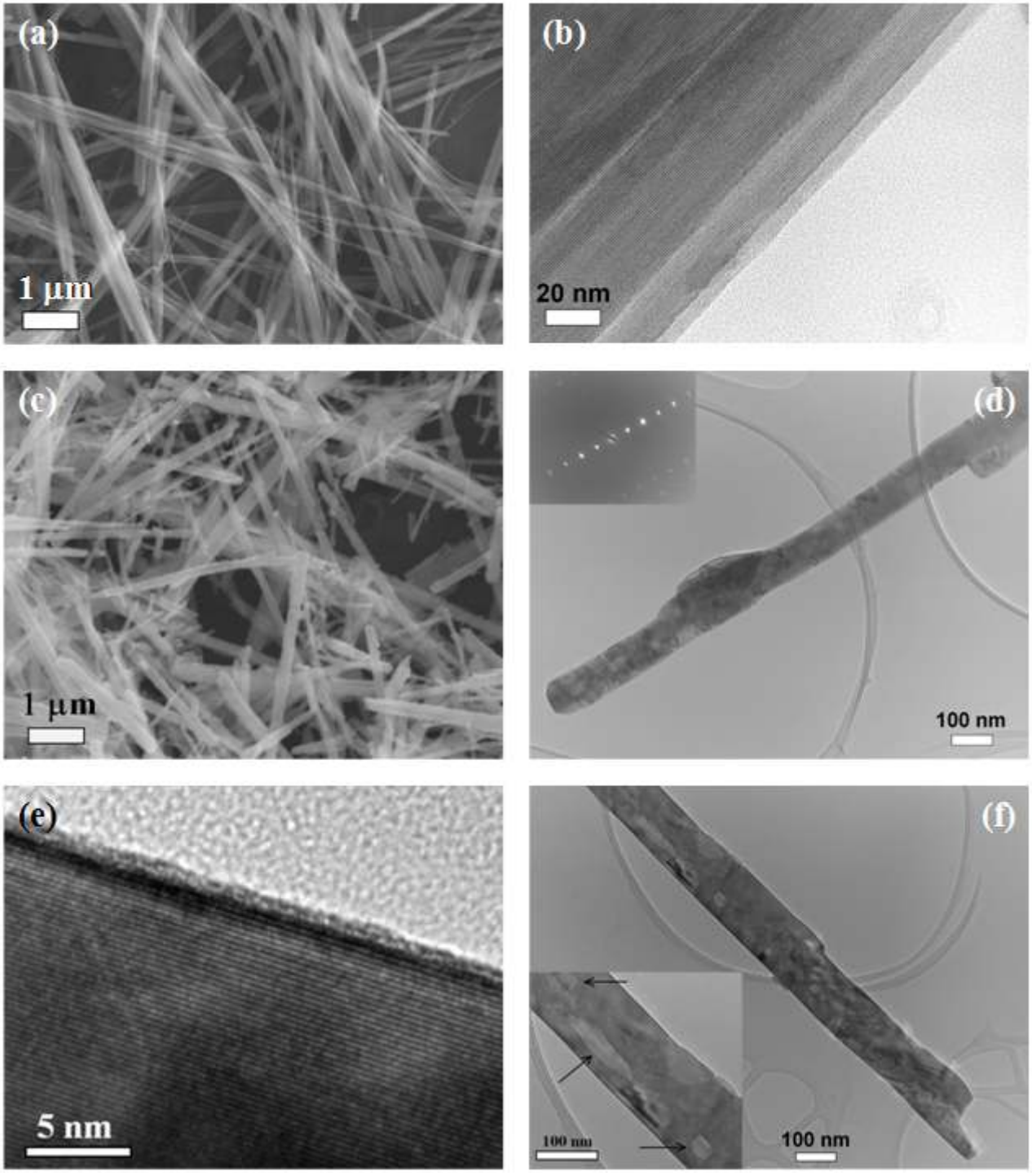

Figure 6. Morphology of titania nanowires: (a) SEM, (b) HRTEM and morphology of $BaTiO_3$ nanowires, (c) SEM, (d-f) TEM and HRTEM. The inset of part (d) shows the ED pattern of the nanowire. The inset of part (f) evidences some defects.

tion corresponds to rather short reaction time, whereas in the range 6–24 h the Bi titanate moved towards a predominant tetrahedral morphology. When Bi_2O_3 was employed, microscopic observations provide evidence that nanowires are very thin with a diameter of about 10–13 nm. On the contrary, if TTB is used, the reaction yielded rather large nanosheets.

These results shown that NaOH plays a very important role in hydrothermal synthesis of Bi titanate. In fact, when the molarity of NaOH increases, a strong change oh morphology results as the production of nanowires in strongly reduced. Also the reaction time seems to be a factor of morphological difference: a quite noticeable variation was observed when the reaction is carried out from 12 to 48 where an almost complete conversion of Bi_2O_3 to uniform lamellar structure of $Bi_4Ti_3O_{12}$ was observed (Fig. 7c,d).

IV. Conclusions

Oriented aggregation represents a fascinating and powerful tool to design and realise materials with desired shape, anisotropy and properties. It is expected that the self-assembly process might be directed to the production of a range of shapes and architectures by the use of organic molecules or polymers that selectively adsorb on specific solid surfaces and/or by employing suitable templates. Core-shell particles represent a useful approach to design and realise new and more complex materials with improved or even innovative functionality. The process of precipitation from solution is mainly driven by electrostatic interactions and is particularly well suited for coating BT or BC submicron particles with a shell of a different compound. This approach can be used as an alternative to mechanical wet mixing for controlled doping of ferroelectric materials and for the fabrication of composite materials with specific geometry of the two phase assembly. We succeeded to directly grow a shell of ST onto the surface of BT spherical templates by means of a precipitation process making use of inorganic precursors. The overall composition and the particle size can be tailored over a wide range. Homogeneous and smooth coatings of $Y(OH)CO_3$ that turn into Y_2O_3 by thermal treatment. More complex composites with a magnetic core of ferrite or hematite and BT shell were produced by a two step coating followed by a solid state reaction between the two layers. The combination of magnetic and ferroelectric phases represents a suitable route to design and produce new multiferroic composites. The present meth-

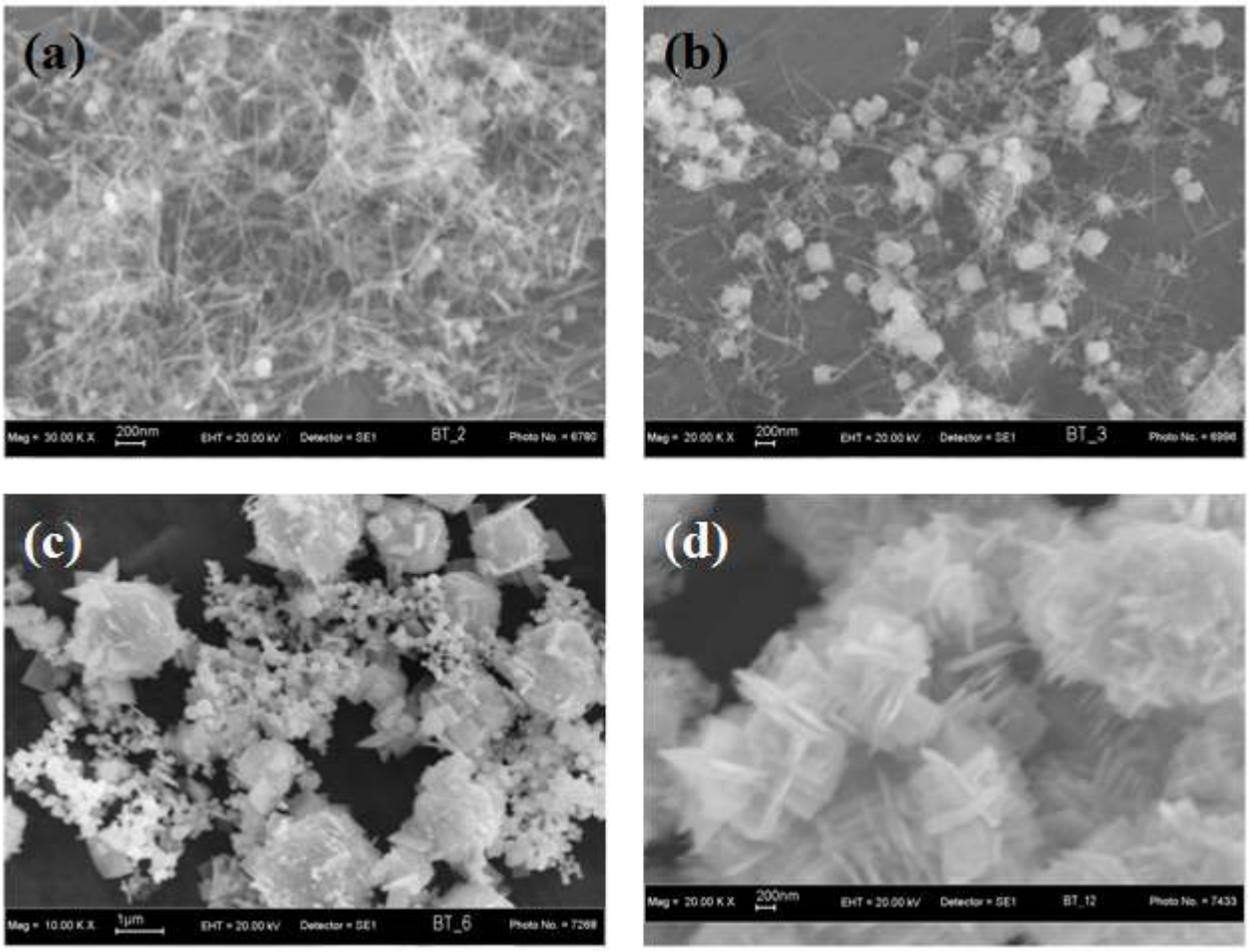

Figure 7. SEM images of $Bi_4Ti_3O_{12}$ powders as function of NaOH concentration and time (NaOH 1 M, 200°C: a) 12 h, b) 24 h; NaOH 5 M, 200°C: c) 24 h, d) 48 h)

od was also extended to basic carbonate coatings of other rare-earths. Core-shell particles can be versatile precursors also for solid-state synthesis of materials with unusual morphology. A new two-step method for the fabrication of hollow $BaTiO_3$ ferroelectric particles was designed. $BaCO_3$ crystals were first coated with a shell of amorphous TiO_2 by means of a precipitation process and then the resulting core-shell particles were converted into $BaTiO_3$ hollow particles by calcination due to the much faster out-diffusion mechanism of the core phase as compared with the in-diffusion of the shell material. Barium titanate nanowires were obtained by solid-state reaction at 700°C using titania fiber-like crystals coated with $BaCO_3$ nanoparticles. The morphology of the titania precursor was retained during the reaction with formation of single-crystal $BaTiO_3$ nanowires. Based on the SEM and TEM results, we propose that formation of barium titanate occurs by a topochemical reaction. Therefore, the titania nanowires not only serve as reactant, but can be considered as reactive templates. Regarding $Bi_4Ti_3O_{12}$, we are trying to tune a single morphology of ferroelectric nanomaterial of bismuth titanate. Up to the moment, $Bi_4Ti_3O_{12}$ nanoplates were synthesised by PEG assisted hydrothermal method at temperature of 200°C for 48 h with single crystalline phase of titanate. It has been found that both temperature and NaOH molarity play a very important role in the formation of well defined confined nanostructures. Our study mainly provides a new method to direct growth of platelets nanostructure and related material. An attempt to retrieve some nanoscale information of these platelets and to find out domain structure is in progress.

Acknowledgements: The collaboration within the COST Action 539 is greatfully recognised. The financial support of the Romanian grant CNCSIS-IMECOMP (PN II_RU_TE_187/2010) is also acknowledged.

References

1. K. Uchino, *Ferroelectric Devices*, Marcel Dekker, Inc., New York, 2000.
2. J.F. Scott, F.D. Morrison, M. Miyake, P. Zubko, X. Lou, V.M. Kugler, S. Rios, M. Zhang, T. Tatsuta, O. Tsuji, T.J. Leedham, "Recent materials characterizations of [2D] and [3D] thin film ferroelectric structures", *J. Am. Ceram. Soc.*, **88** (2005) 1691–1701.
3. N. Setter, L. Eng, G. Fox, S. Gevorgian, S. Hong, A. Kingon, H. Kohlstedt, N.Y. Park, G.B. Stephenson, I. Stolitchnov, A.K. Tagantsev, D.V. Taylor, T. Yamada, S. Streifer, "Ferroelectric thin films: Review of materials, properties, and applications", *J. Appl. Phys.*, **100** (2006) 051606.
4. A.K. Tagantsev, V.O. Sherman, K.F. Astafiev, J. Venkatesh, N. Setter, "Ferroelectric materials for microwave tunable applications" *J. Electroceram.*, **11** (2003) 5–66.
5. A. Rüdiger, T. Schneller, A. Roelofs, S. Tiedke, T. Schmitz, R. Waser, "Nanosize ferroelectric oxides -tracking down the superparaelectric limit", *Appl. Phys. A.*, **80** (2005) 1247–1255.
6. X.H. Zhu, P.R. Evans, D. Byrne, A. Schilling, C. Douglas, R.J. Pollard, R.M. Bowman, J.M. Gregg, F.D. Morrison, J.F. Scott, "Perovskite lead zirconium titanate nanorings: towards nanoscale ferroelectric "solenoids"?", *Appl. Phys. Lett.*, **89** (2006) 122913–122915.
7. A. Schilling, R.M. Bowman, G. Catalan, J.F. Scott, J.M. Gregg, "Morphological control of polar orientation in single-crystal ferroelectric nanowires", *Nano Lett.*, **7** (2007) 3787–3791.
8. I.I. Naumov, L. Bellaiche, H. Fu, "Unusual phase transitions in ferroelectric nanodisks and nanorods", *Nature*, **432** (2004) 737–740.
9. H. Fu, L. Bellaiche, "Ferroelectricity in barium titanate quantum dots and wires", *Phys. Rev. Lett.*, **91** (2003) 257601.
10. J.F. Scott, "Ferroelectrics: Novel geometric ordering of ferroelectricity", *Nature Mater.*, **4** (2004) 13–14.
11. S-B. Cho, M. Oledzka, R.E. Riman, "Hydrothermal synthesis of acicular lead zirconate titanate (PZT)", *J. Cryst. Growth*, **226** (2001) 313–326.
12. G. Suyal, E. Colla, R. Gysel, M. Cantoni, N. Setter, "Piezoelectric response and polarization switching in small anisotropic perovskite particles", *Nano Lett.*, **4** (2004) 1339–1342.
13. G. Xu, Z.H. Ren, P.Y. Du, W.J. Weng, G. Shen, G.R. Han, "Polymer-assisted hydrothermal synthesis of single-crystalline tetragonal perovskite $PbZr_{0.52}Ti_{0.48}O_3$ nanowires", *Adv. Mater.*, **17** (2005) 907–910.
14. J. Wang, C.S. Sandu, E. Colla, Y. Wang, W. Ma, R. Gysel, H.J. Trodahl, N. Setter, "Ferroelectric domains and piezoelectricity in monocrystalline $Pb(Zr,Ti)O_3$ nanowires", *Appl. Phys. Lett.*, **90** (2007) 133107.
15. J.J. Urban, W.S. Yun, Q. Gu, H. Park, "Synthesis of single-crystalline perovskite nanorods composed of barium titanate and strontium titanate", *J. Am. Chem. Soc.*, **124** (2002) 1186–1187.
16. W.S. Yun, J.J. Urban, Q. Gu, H. Park, "Ferroelectric properties of individual barium titanate nanowires investigated by scanned probe microscopy", *Nano Lett.*, **2** (2002) 447–450.
17. J.J. Urban, J.E. Spanier, O.Y. Lian, W.S. Yun, H. Park, "Single-crystalline barium titanate nanowires", *Adv. Mater.*, **15** (2003) 423–426.
18. U.A. Joshi, J.S. Lee, "Template-free hydrothermal synthesis of single-crystalline barium titanate and strontium titanate nanowires", *Small*, **1** (2005) 1172–1176.
19. U.A. Joshi, S. Yoon, S. Baik, J.S. Lee, "Surfactant-free hydrothermal synthesis of highly tetragonal barium titanate nanowires: a structural investigation", *J. Phys. Chem. B*, **110** (2006) 12249–12256.
20. Z. Wang, M-F. Yu, "One-dimensional ferroelectric monodomain formation in single crystalline $BaTiO_3$ nanowire", *Appl. Phys. Lett.*, **89** (2006) 263119.

21. S-O. Kang, BH. Park, Y-I. Kim, "Growth mechanism of shape-controlled barium titanate nanostructures through soft chemical reaction", *Cryst. Growth. Des.*, **8** (2008) 3180–3186.
22. H.J. Fan, U. Gösele, M. Zacharias, "Formation of nanotubes and hollow nanoparticles based on Kirkendall and diffusion processes: A review", *Small*, **3** (2007) 1660–1671.
23. C. Bae, H. Yoo, S. Kim, K. Lee, J. Kim, M.M. Sung, H. Shin, "Template-directed synthesis of oxide nanotubes: fabrication, characterization, and applications", *Chem. Mater.*, **20** (2008) 756–767.
24. H.J. Fan, M. Knez, R. Scholz, K. Nielsch, E. Pippel, D. Hesse, M. Zacharias, U. Gösele, "Monocrystalline spinel nanotube fabrication based on the Kirkendall effect", *Nature Mater.*, **5** (2006) 627–631.
25. Y. Yang, R. Scholz, H.J. Fan, D. Hesse, U. Gösele, M. Zacharias, "Multitwinned spinel nanowires by assembly of nanobricks via oriented attachment: a case study of Zn_2TiO_4", *ACS Nano*, **3** (2009) 555–562.
26. M.T. Buscaglia, M. Viviani, Z. Zhao, V. Buscaglia, P. Nanni, "Synthesis of $BaTiO_3$ core-shell particles and fabrication of dielectric ceramics with local graded structure", *Chem. Mater.*, **18** (2006) 4002–4010.
27. N. Kawahashi, E. Matijevic, "Preparation and properties of uniform coated colloidal particles: V. Yttrium basic carbonate on polystyrene latex", *J. Colloid. Interface Sci.*, **138** (1990) 534–542.
28. A. Bassano, V. Buscaglia, M. Sennour, M.T. Buscaglia, M. Viviani, P. Nanni, "Nanocrystalline oxide (Y_2O_3, Dy_2O_3, ZrO_2, NiO) coatings on $BaTiO_3$ submicron particles by precipitation", *J. Nanopart. Res.*, (2009) DOI 10.1007/s11051-009-9631-0.
29. M.T. Buscaglia, V. Buscaglia, M. Viviani, G. Dondero, S. Röhrig, A. Rüdiger, P. Nanni, "Ferroelectric hollow particles obtained by solidstate reaction", *Nanotechnol.*, **19** (2008) 225602.
30. M.T. Buscaglia, C. Harnagea, M. Dapiaggi, V. Buscaglia, A. Pignolet, P. Nanni, "Ferroelectric $BaTiO_3$ nanowires by a topochemical solid-state reaction", *Chem. Mater.*, **21** (2009) 5058–5065.
31. V.R. Calderone, A. Testino, M.T. Buscaglia, M. Bassoli, C. Bottino, M. Viviani, V. Buscaglia, P. Nanni, "Size and shape control of $SrTiO_3$ particles grown by epitaxial self-assembly", *Chem. Mater.*, **18** (2006) 1627–1633.
32. B. Aiken, W.P. Hsu, E. Matijevic, "Preparation and properties of monodispersed colloidal particles of lanthanide compounds: III. Yttrium(III) and mixed yttrium(III)/cerium(III) systems", *J. Am. Ceram. Soc.*, **71** (1988) 845–853.
33. M.T. Buscaglia, V. Buscaglia, R. Alessio, "Coating of $BaCO_3$ crystals with TiO_2: Versatile approach to the synthesis of $BaTiO_3$ tetragonal nanoparticles", *Chem. Mater.*, **19** (2007) 711–718.
34. C-C. Tsai, H. Teng, "Structural features of nanotubes synthesized from NaOH treatment on TiO_2 with different posttreatments", *Chem. Mater.*, **18** (2006) 367–373.
35. S.K. Pradhan, Y. Mao, S.S. Wong, P. Chupas, V. Petkov, "Atomic-scale structure of nanosized titania and titanate: Particles, wires, and tubes", *Chem. Mater.*, **19** (2007) 6180–6186.